Int. Conf. on Ultra Wideband Systems and Technologies, pp. 86-90, November 2003, Reston, Virginia

A FREQUENCY-DOMAIN APPROACH FOR ALL-DIGITAL CMOS ULTRA WIDEBAND RECEIVERS

Hyung-Jin Lee[1], Dong Sam Ha[1], and Hyung-Soo Lee[2]

[1]VTVT (Virginia Tech VLSI for Telecommunications) Lab
Department of Electrical and Computer Engineering
Virginia Tech, Blacksburg, VA 24061
E-mail: {hlee, ha}@vt.edu

[2]Radio and Broadcasting Laboratory
Electronics and Telecommunications Research Institute
Yuseong-Gu, Daejon Korea
E-mail: hsulee@etri.re.kr

Abstract – In this work, we propose a new approach to process received signals in the frequency-domain, which opens the possibility for CMOS implementation of all-digital ultra wideband receivers. The key idea for the proposed method is to extract the frequency components of the received signal and to perform signal processing in the frequency domain. The proposed receiver architecture relaxes the speed requirement of analog-to-digital converters and is highly suitable for a multipath rich environment such as UWB. Our simulation results indicate that the proposed receiver improves the SNR by about 3 dB at BER=10^{-1} when compared with an analog receiver under multi-path channel conditions.

Index terms: UWB, UWB receiver, Frequency domain, CMOS receiver, Rake receiver

I. INTRODUCTION

The increasing demand for high data rate communication systems has brought the resurrection of ultra wideband (UWB) technology. CMOS implementation of UWB receivers is highly desirable for many UWB applications, in which low cost and/or low-power consumption is critical. However, the wideband nature of UWB leads to a major challenge for CMOS implementation of UWB receivers. The challenge stems from the fact that UWB is based on narrow pulses, and over-sampling of such pulses requires extremely high-speed analog-to-digital converters (ADCs). For this reason, all existing UWB receivers for high data rate rely on analog correlators [1]. Time domain processing using analog correlators prevents the receiver from fully exploiting the advantages of digital communications and results in a low data rate.

The digital UWB receiver in [2] proposes a parallel ADC structure to over-sample received signals within the time period of the interest. However, the approach requires a large number of ADCs. Also, it suffers from a timing-jitter problem, since multiple clocks driving the ADCs are skewed by a fine increment of delay and distribution of such clocks is problematic. A sampling rate conversion technique using multi-channel ADCs was proposed in [3]. The approach requires low speed ADCs, but needs a large number of ADCs for high data rate. We proposed a frequency domain approach in [4] to address the problem, and this paper extends and refines our earlier work.

II. BACKGROUND

In this section, we describe two important concepts employed for our proposed receiver design.

A. SIGNAL ANALYSIS IN FREQUENCY-DOMAIN

A continuous-time periodic signal with a period T_p is expressed as

$$x(t) = \sum_{k=-\infty}^{k=\infty} c_k e^{j2\pi k F_0 t} \tag{1}$$

$$c_k = \frac{1}{T_p}\int_{T_p} x(t) e^{-j2\pi k F_0 t} dt \tag{2}$$

where $F_0 = 1/T_p$ is the fundamental frequency of the signal $x(t)$, and a coefficient c_k represents a spectral component of the signal. Note that c_k's are usually complex values, and c_k and c_{-k} are complex conjugate. A period T_p is the observation window of the received signal, which is often a fraction of the pulse repetition interval (PRI).

Noting $\omega_0 = 2\pi F_0 = \dfrac{2\pi}{T_p}$ and using the periodic characteristics of a sinusoidal function, (2) leads to the relation given in (3).

$$c_k = \frac{1}{T_p}\left[\int_{T_p} x(t)\cos(kw_0 t)dt - j\int_{T_p} x(t)\sin(kw_0 t)dt\right]$$
$$= \frac{1}{T_p}\left[\int_{T_p} x(\tau)\cos(kw_0(T_p-\tau))d\tau + j\int_{T_p} x(\tau)\sin(kw_0(T_p-\tau))d\tau\right]$$
$$= \frac{1}{T_p}\left[x(t)*\cos(k\omega_0 t) + jx(t)*\sin(k\omega_0 t)\big|_{t=T_p}\right] \qquad (3)$$

where k is integer and '*' is the convolution operation.

Noting

$$L\{\cos(k\omega_0 t)\} = \frac{s}{s^2+(k\omega_0)^2},\quad L\{\sin(k\omega_0 t)\} = \frac{k\omega_0}{s^2+(k\omega_0)^2}$$

where $L\{\}$ represents Laplace transform.

(3) can be expressed as following.

$$c_k = \frac{1}{T_p}\left(X(s)\frac{s}{s^2+(k\omega_0)^2} + jX(s)\frac{k\omega_0}{s^2+(k\omega_0)^2}\Bigg]_{s=2\pi f}\right) \qquad (4)$$

where $X(s)$ is Laplace transform of $x(t)$. (4) provides necessary background for the proposed frequency domain approach, and implementation of (4) in hardware is described in the next section.

B. SAMPLING THEOREM REVISITED

If a continuous-time periodic signal $x(t)$ is *band limited,* its Fourier coefficient $c_k=0$ for $|k|>M$ as shown in Figure 1(a), where M is a positive integer. Similarly, if a Fourier coefficient $c_k=0$ for $M<|k|<N/2$ and the sampling frequency $f_s = NF_0$ as shown in Figure 1 (b), a periodic discrete-time signal has the fundamental period N in time domain and is periodically band limited. Suppose that the sampling frequency $f_s = F_s = NF_0$ (which implies N samples during the fundamental period T_p) in Figure 1 (b), the resolution of spectral components $2\pi/N$ is equivalent to F_0 due to the relationship of $\frac{2\pi}{N} \equiv \frac{f_s}{N} = \frac{NF_0}{N} = F_0$. Note that the normalized frequency 2π corresponds to $f_s=F_s=NF_0$.

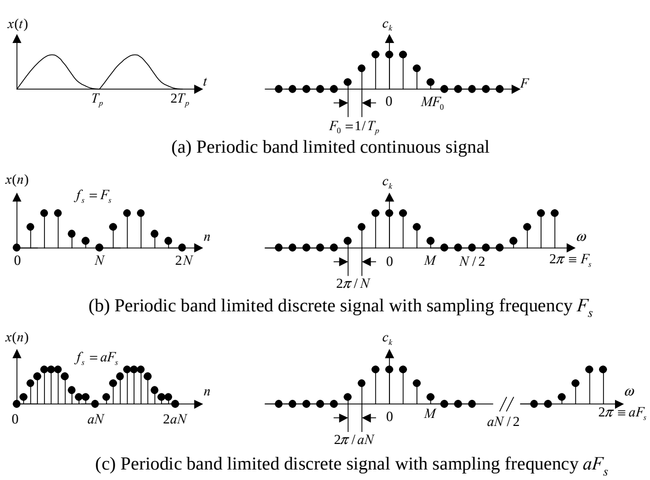

(a) Periodic band limited continuous signal

(b) Periodic band limited discrete signal with sampling frequency F_s

(c) Periodic band limited discrete signal with sampling frequency aF_s

Figure 1: Signals in time and frequency domains

In the same manner, the resolution of the spectral components for the signal in Figure 1 (c) is $2\pi/aN$ for the sampling frequency $f_s=aF_s=aNF_0$. However, the resolution of the spectral components still remains the same F_0 due to the relationship of $\frac{2\pi}{aN} \equiv \frac{f_s}{aN} = \frac{aNF_0}{aN} = F_0$. An important fact is that the Fourier coefficient c_k for all the three signals in the figure is identical for $|k|\le M$. This suggests that the sampling rate of a band limited periodic signal can be increased by simply padding zeros. We exploit this property to increase the sampling rate of the received signal.

III. FREQUENCY-DOMAIN PROCESSING

In this section, we present a frequency domain sampler and describe the convolution and correlation operations in the frequency domain.

A. FREQUENCY DOMAIN SAMPLING

Expression (3) and (4) imply that a coefficient c_k can be obtained by sampling the outputs of analog filters with transfer functions of $\frac{1}{s^2+(k\omega_0)^2}$ and of $\frac{s}{s^2+(k\omega_0)^2}$. The filter with a transfer function of $\frac{1}{s^2+(k\omega_o)^2}$ can be implemented using an LC resonator, and the factor of '**s**' is a differentiator. The structure of a filter bank is shown in Figure 2, and a filter bank captures one spectral component of the received signal.

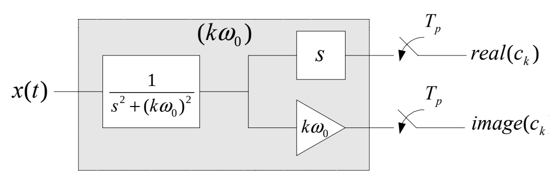

Figure 2: A filter bank

A frequency-domain sampler consists of multiple filter banks followed by multiple ADCs as shown in Figure 3. Each filter bank f_i captures the spectral component of the frequency f_i of the received signal, where $f_i = kF_0$ for an integer k. Further, f_i should reside in the in-band spectrum. Note that f_0 is not necessarily the same as the fundamental frequency F_0. The number of filter banks is determined by a time-window size T_p. A larger time window captures more multipaths, but it decreases the fundamental frequency F_0, which, in turn, increases the total number of filter banks.

Each filter bank requires two ADCs and the sampling rate of the ADCs is the inverse of the PRI. A salient point of the proposed frequency domain sampler is that the ADC speed is determined by the PRI, not the over-sampling rate and the width of received pulses. So ADCs operate much a lower frequency to enable CMOS implementation of ADCs. Note that ADCs can be time-shared provided the ADC speed allows several samples within a PRI.

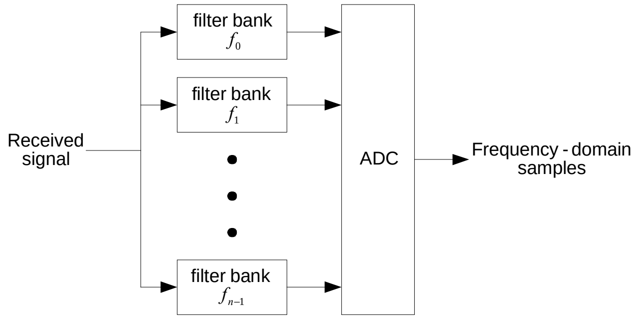

Figure 3: Frequency-domain sampler

B. TIME-DOMAIN SIGNAL RECONSTRUCTION

It is possible to reconstruct a sampled signal in the time domain from spectral components obtained from the frequency-domain sampler. This can be done by performing an IFFT (Inverse Fast Fourier Transform) operation of the spectral components with an adequate number of zeros padded. Note that the sampling frequency is determined by the number of zeros padded. Figure 4 shows a time-domain signal reconstructed through a 128-point IFFT, in which the time-window size is 1 ns, the number of filter banks is seven, and 114 zeros are padded. The reconstructed signal is close to the original signal, especially during the main portion of the pulse (whose spectrum is mostly in-band). The discrepancy between the original signal and the reconstructed one is due to the elimination of out-band spectral components, which is not a concern.

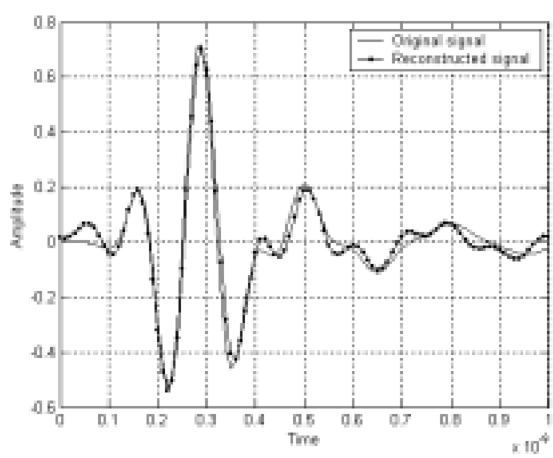

Figure 4: Reconstructed time-domain signal

C. CORRELATION AND CONVOLUTION

A correlation operation of two real signals *x(t)* and $\tilde{x}(t)$ in time domain is indeed a multiplication in frequency domain as expressed below.

$$R(\tau) \equiv \int x(t)\tilde{x}(t+\tau)dt = F^{-1}\{X^*(f)\tilde{X}(f)\} \tag{5}$$

The peak correlation value for a received signal and the template occurs at $\tau=0$ in the time domain if the receiver and transmitter are perfectly synchronized. The correlation value at $\tau=0$ is equivalent to the index-0 output of an IFFT block, which is the sum of the entire spectral components, i.e., all the multiplication results. In a similar manner, the convolution operation in the time domain is also a multiplication in the frequency domain. Hence, correlation and convolution operations can be performed efficiently in the frequency domain.

IV. ARCHITECTURE OF THE PROPOSED UWB RECEIVERS

Our frequency domain approach described earlier enables processing of the received signals in the frequency domain and can be applied to any communication system, including narrowband systems. In this section, we present an architecture for impulse-based UWB receivers employing the frequency domain approach.

A. OVERALL RECEIVER ARCHITECTURE

Figure 5 shows the overall architecture for impulse-based UWB radios using the frequency domain approach. The proposed UWB receiver consists of multiple narrowband LNAs (Low Noise Amplifiers), a frequency domain sampler, an energy harvester block, and a decision block.

It is possible to use one wideband LNA for our receiver, but a wideband LNA is difficult to implement in CMOS. The other extreme is to assign one narrowband LNA at the front of each filter bank as shown in the figure. The number of LNAs can be adjusted properly considering the circuit complexity and ease of CMOS implementation.

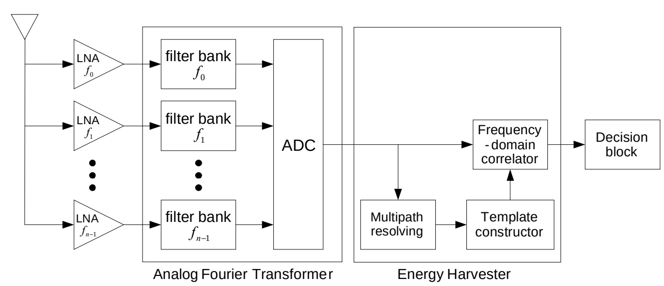

Figure 5: Proposed UWB receiver architecture

The energy harvester block collects the energy dispersed on multipaths, and its function is identical to the rake function used for narrowband communications systems. The multipath resolving block identifies multipaths through a series of operations. A new template signal based on the resolved multipath signals is generated and is correlated with the received signal to collect the energy on multipaths. The proposed energy harvester is more effective and much simpler in hardware than a conventional rake receiver as is explained later.

B. ENERGY HARVESTER

The energy harvester performs three operations, identification of multipaths, generation of a dynamic template, and collection of the energy dispersed on multipaths. Multipaths can be identified from the correlation operation in the time domain as follows. A received signal is correlated with a static template signal (derived based on a single transmitted pulse) through multiplication in the frequency domain. An IFFT with a zero padding is performed on the result to obtain the correlation function $R(\tau)$ in the time domain, and the waveform of $R(\tau)$ is illustrated in Figure 6. Under the assumption that a multipath exists provided $R(\tau)$ exceeds a threshold value, the impulse response of the channel is estimated by identifying all multipaths.

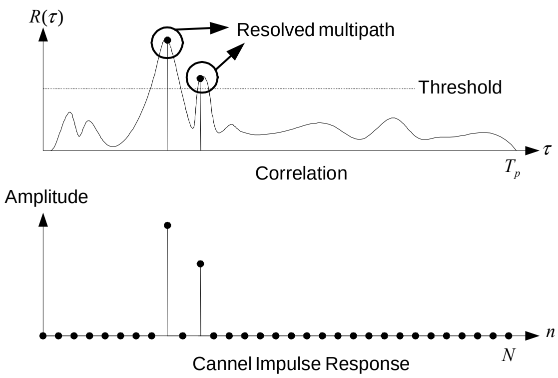

Figure 6: Channel impulse response formation

A new dynamic template is generated based on the impulse response of the estimated channel by convolving the impulse response of the channel with a static template signal as shown in Figure 7. To exploit the simplicity of the convolution operation (which is a multiplication) in the frequency-domain, the impulse response of the estimated channel is translated back into frequency domain through FFT first, and then a dynamic template is obtained in the frequency domain by multiplying spectral components of the impulse response and the static template.

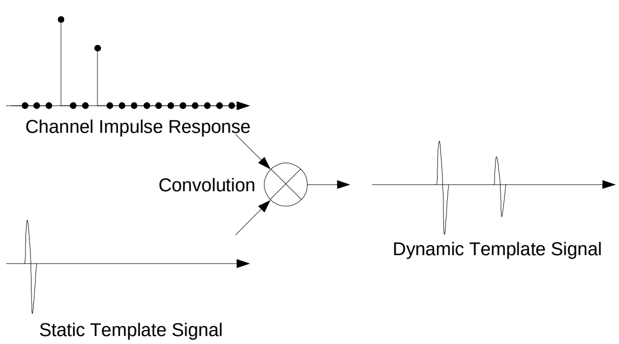

Figure 7: Dynamic template generation

Once a dynamic template is generated, the energy of the multipaths is collected by correlating a received signal with the dynamic template. The energy collection process is explained below. The received signal $x(t)$ with multipaths is represented as (6) in the time-domain. Assume that the dynamic template $\tilde{x}(t)$ has identified all the multipaths and can be expressed in (7).

$$x(t) = a_0 p(t_0) + a_1 p(t_0 + \tau_1) + \ldots \quad (6)$$

$$\tilde{x}(t) = a_0 \tilde{p}(t_0) + a_1 \tilde{p}(t_0 + \tau_1) + \ldots \quad (7)$$

where a_i is the gain term, $p(t)$ is the function of the single pulse, t_0 is the arrival time of the first multipath signal, and τ_k is the delay from the first multipath. Hence, the correlation between the received signal and the dynamic template signal at $\tau=0$ is given in (8).

$$\begin{aligned} R(0) &= R(\tau)\big|_{\tau=0} \\ &= \int_{-\infty}^{\infty} a_0^{\,2} p(t_0)\tilde{p}(t_0)dt + \int_{-\infty}^{\infty} a_1^{\,2} p(t_0+\tau_1)\tilde{p}(t_0+\tau_1)dt + \ldots \end{aligned} \quad (8)$$

Note that each term is the energy of the multipath, and $R(0)$ is sum of the individual energy

C. COMPARISON WITH A RAKE STRUCTURE

A conventional narrowband digital receiver employs a rake receiver to exploit multipaths constructively. Since it requires one finger to process one multipath signal, the maximum number of manageable multipaths is fixed by the number of fingers. Moreover, the circuit complexity increases rapidly as the number of fingers increases. In contrast, the proposed energy harvester processes all multipaths, and its circuit complexity is independent of the number of multipaths. Therefore, it is highly desirable for a multipath rich environment such as UWB. Lastly, a conventional rake structure needs de-skewing process to adjust delays between multipaths, while the proposed energy harvester does not to result in further reduction of the circuit complexity.

V. SIMULATION RESULT

In this section, we present simulation results for the performance of the proposed frequency domain UWB receiver and compare the results with conventional UWB receivers employing analog correlators. Two receivers, one for the single-band covering the entire spectrum allocated by the FCC [5] and the other one covering only the lower-band, were modeled in Matlab and were simulated for Intel channel model [6]. The system specifications of the two receivers are as follows.

Single-band UWB receiver:

- Pulse width: 145 ps
- Bandwidth: 7.5 GHz (3.1 GHz – 10.6 GHz)
- Pulse shaping: Band-pass filtered Gaussian monocycle pulse
- PRI: 10 ns
- Number of filter banks: 7
- Time window size: 1 ns

Lower-band UWB receiver:

- Pulse width: 242 ps
- Bandwidth: 2.08 GHz (3.1 GHz – 5.18 GHz)
- Pulse shaping: Band-pass filtered Gaussian monocycle pulse
- PRI: 10 ns
- Number of filter banks: 6
- Time window size: 3 ns

Note that channel coding was not employed for the receivers.

Figure 8 shows simulation results for the single-band UWB receivers. The simulation results indicate that the proposed receiver performs better than the analog receiver for the entire range of the SNR simulated, and the performance gap increases with increase of the SNR. The proposed receiver improves the SNR by 3.5 dB at BER=10^{-1} when compared with the analog receiver. The better performance is attributed to the harvest of multipath energy for our receiver.

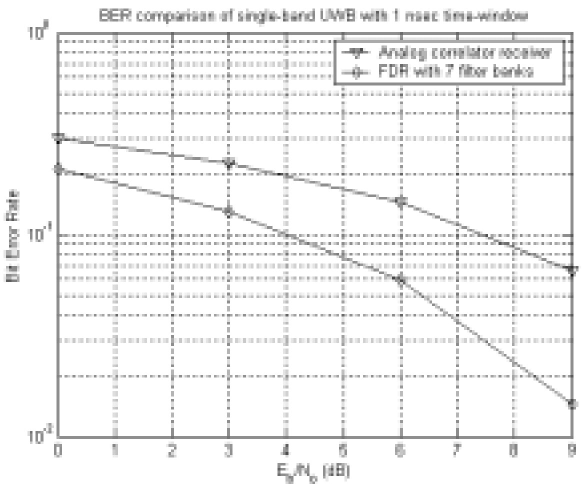

Figure 8: Performance of the single band UWB receivers

Figure 9 shows the performance for lower-band receivers. Like single-band receivers, the proposed receiver performs better than the analog receiver for the entire range of the SNR experimented. The performance improvement of the proposed receiver is about 3 dB at BER=10^{-1} over the analog receiver. Note that the performance of both the proposed and analog lower-band receivers degrades compared with the single-band receivers. This is caused by the increase of the inter-symbol interference due to a wider pulse width for the lower-band receivers.

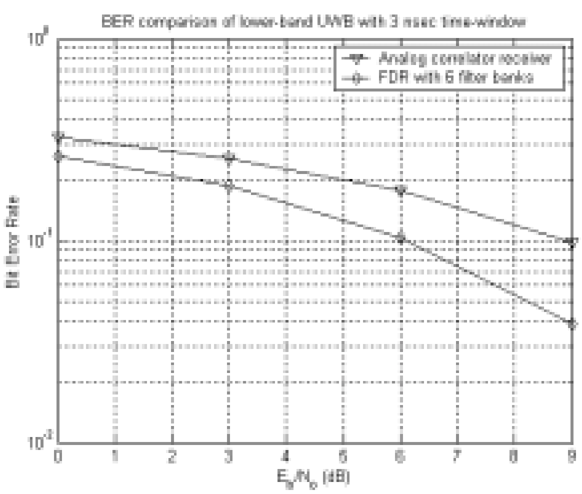

Figure 9: Performance of the lower-band UWB receivers

VI. CONCLUSION

In this paper, we proposed a new UWB receiver architecture based on the frequency domain approach. The proposed frequency domain approach relaxes the speed requirement for ADCs, which is a critical issue for all-digital CMOS UWB receivers. The energy harvester block of the proposed rake receiver is highly suitable for a multipath rich channel such as UWB. In addition, narrowband LNAs can be used for the proposed receiver, which makes our receivers more CMOS friendly.

Further research is needed for efficient implementation of CMOS filter banks and development of efficient DSP algorithms for frequency-domain processing. Finally, we believe that the proposed frequency domain approach has removed the major technical barrier to enable all digital CMOS UWB receivers for high data rate.

VII. REFERENCE

[1] R.A. Scholtz and M.Z. Win, "Impulse Radio," Invited Paper, IEEE PIMRC '97, Helsinki, 1997.

[2] O'Donnell, M. Chen, S. Wang and R. W. Brodersen, "An Integrated, Low-Power, Ultra-Wideband Transceiver Architecture for Low-Rate, Indoor Wireless Systems," IEEE CAS Workshop on Wireless Communications and Networking, September 2002.

[3] C. Gangyaokuang and S. Zhonglianglu, "A Way of Multi-channel A/D for UWB Signal," IEEE NAECON 1995, Vol. 1, pp. 206-209, May 22-26, 1995.

[4] H. J. Lee and D. S. Ha, "Frequency Domain Approach for CMOS Ultra-Wideband Radios," VLSI, 2003 IEEE Computer Society Annual Symposium, pp. 236-237, February 20-21, 2003.

[5] Revision of Part 15 of The Commission's Rules Regarding Ultra Wideband Transmission Systems, FCC 03-33, ET Docket 98-153, February 13 2003.

[6] J. Foerster, "Channel modeling sub-committee report final," IEEE document number #02490r1-SG3a, February 2003.